ANALES de Edificación

Anales de Edificación
Vol. 6, Nº2, 7-19 (2020)
ISSN: 2444-1309
Doi: 10.20868/ade.2020.4491

Received: 23-01-2020
Accepted: 09-02-2020

Componentes Optimizados de Fabricación de Aditivos
Optimized Additive Manufacturing Building Components

Luis Borunda[a], Manuel Ladrón de Guevara[b], Gianluca Pugliese[c], Rafael Claramunt[a], Marta Muñoz[a], Jesús Anaya[a]

[a] Universidad Politécnica de Madrid (lborunda.eco@etsav.catUniversty; rclaramunt@etsii.upm.es; marta.munoz@etsii.upm.es; jesus.anaya@upm.es), [b] Carnegie Mellon University (manuelr@andrew.cmu.edu), [c] Wasp Iberia 3D Printing Services (madrid@wasp3d.es)

***Resumen*— Inicialmente destinadas a la creación rápida de prototipos, las tecnologías de fabricación aditiva se adaptan cada vez más a la producción de componentes funcionales. Su aplicación en arquitectura ha crecido rápidamente desde el lanzamiento público de patentes, la técnica más popular es la técnica AM, Fused Deposition Modeling (FDM), y desde el desarrollo de varias técnicas de producción automatizadas a gran escala. La optimización de las geometrías para FDM es fundamental para aprovechar el potencial de la producción arquitectónica de AM. Esta investigación evalúa los flujos de trabajo computacionales basados en los datos de estructuración en nubes isostáticas que incorporan bucles de retroalimentación de simulación en el diseño de componentes funcionales diferenciando internamente la geometría y la composición del material específicamente adaptando una pieza para una aplicación dada. Esto conduce a un rendimiento mejorado mientras reduce potencialmente, el tiempo de fabricación, el uso del material y, por lo tanto, el impacto ambiental. El método propuesto utiliza los resultados obtenidos del análisis de elementos finitos (FEA) para diseñar componentes de construcción anisotrópicos determinando discretamente las geometrías de relleno. La contribución de esta investigación radica en la creación y corroboración de un flujo de trabajo computacional probado en componentes FDM termoplásticos para evaluar la generalización del método de diseño de estructuras de relleno de ingeniería, la identificación de varias restricciones geométricas debido a limitaciones en las técnicas de deposición y presentar los resultados de pruebas de rendimiento mecánico de diferentes diseños de casos basados en AM para avanzar en la automatización de la producción.**

Palabras Clave— Opimización de topología; fabricación aditiva a gran escala, modelado de deposición fundida; análisis de elementos finitos.

***Abstract*— Initially intended for Rapid Prototyping, Additive Manufacturing technologies are increasingly being adapted to functional component production. Its application in architecture has been quickly growing since the public release of patents the most popular AM technique, Fused Deposition Modelling (FDM), and since the development of several large-scale automated production techniques. The optimization of geometries for FDM is critical to harness the potential of AM architectural production. This research assesses computational workflows based on the structuring data in isostatic clouds that incorporate simulation feedback loops in the design of functional components by internally differentiating the geometry and material composition specifically tailoring a piece for a given application. This leads to improved performance while potentially reducing, fabrication time, material use, and therefore, environmental**

L. Borunda, R. Claramunt, M. Muñoz, J. Anaya pertenecen a la Escuela Técnica Superior de Arquitectura de la Universidad Politécnica de Madrid
M. Ladrón de Guevara pertenece a la Carnegie Mellon University: School of Architecture.
G. Pugliese pertenece a la Wasp Iberia 3D Printing Services.

impact. The proposed method uses results attained from Finite Element Analysis (FEA) to engineer anisotropic building components by discretely determining infill geometries. The contribution of this research lies in the creation and corroboration of a computational workflow tested on thermoplastic FDM components to assess the generalizability of the design method of engineering infill structures, the identification of several geometrical constraints due to limitations in deposition techniques and to present the results of mechanical performance tests of different AM based designs case studies to advance production automation.

Index Terms— Topology Optimization; Large Scale Additive Manufacturing; Fused Deposition Modelling; Finite Element Analysis.

I. Introducción

Additive manufacturing (AM) has seen an exponential growth of application In architecture and construction since the release of several technique patents. Among the most commonly used AM techniques in architecture is Fused Deposition Modeling (FDM), a process based in the numerical control deposition of a plastic material (Malé, 2016).

The purpose of this research is to explore where are we heading regarding construction automation by additive manufacturing, particularly exploring the potential of layer by layer Fused Deposition Modelling applications in manufacturing of large scale functionally graded components (figure 1).

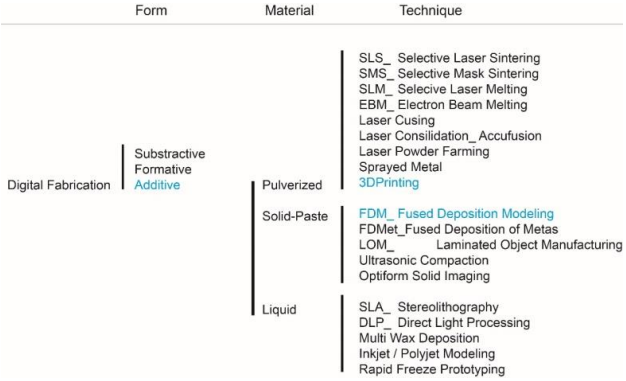

Fig. 1. Digital Fabrication and common Additive Manufacturing techniques.

A. *Robotic Manufacturing and Large Scale FDM*

After important developments in layer by layer principle of manufacturing, such as advances in industrial grade deposition systems and advances in material engineering, the technique is currently being exploited in an increasing amount of architectural projects. Computational methods of utilizing Finite Element Method (FEM) analysis to optimize components by engineering the internal material distribution based on complex three dimensional patterns (3D infills) are presented (figure 2).

B. *Functionally graded building components*

Digital design affords the fundamental act of accessing indexed information and providing unique qualities to individual cells (Oxman. and Rosenberg, 2007; Carpo, 2017). The value of the digital in form can be harnessed with the use of numeric control and robotic manufacturing processes, so that a data unit can have unique characterization in physical materialization (Figure 3). The capacity to access and process data is not only changing the traditional means of form design but also its construction.

Fig. 2. WASP 3MT printer. Thermoplastic pellet extruder for Large Scale AM applications.

Influencing the infill design using FEM Analysis is a current topic research (Tam and Mueller, 2017). The approach presented in this paper evaluates the potential use of strategies common in bone development, density variation and characterization of mechanical performance along the principal

stress lines. AM techniques such as FDM show exceptional capacities of producing very complex structures.

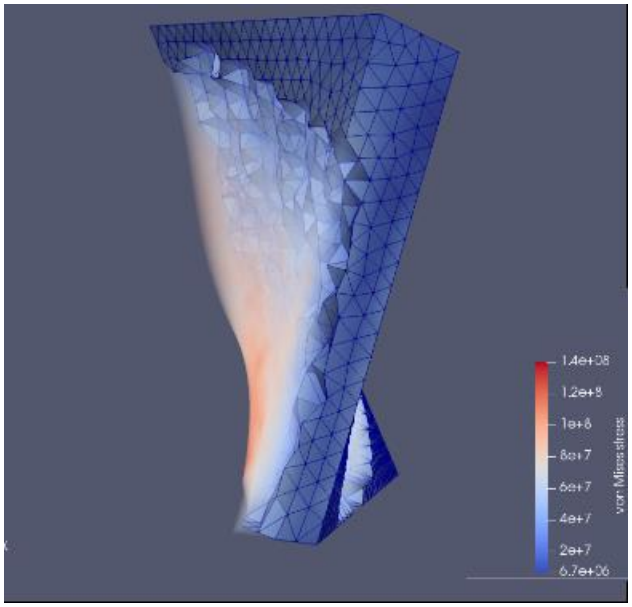

Fig. 3. Low strain VTK cells selected and processed in Paraview.

Although FDM is characterized for anisotropic mechanical behavior (Ahn et al, 2002), varying locally deposition during FDM based on FEM simulation has demonstrated successful transformation of mechanical properties (Gospill et al., 2017).

The characterization of fibrous structures that perform as cellular solids based uniquely on their geometrical difference provides further insight in the use of several types of infills for different large scale application (Figure 4).

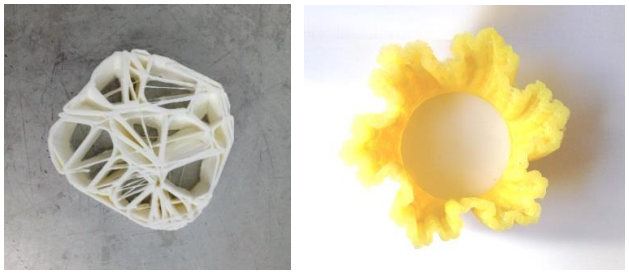

Fig. 4. Custom 3D infill designs and improved Shell design in functionally graded components.

II. METHODS

Experimental devices are divided into several infill geometry tests and one large scale application test.

For this first part of the research 3D printed samples of Triply Periodic Minimal Surfaces (TPMS) (Yoo, 2011) are designed, produced and tested for compression performance and characterization of mechanical properties.

1) First step is to evaluate manufacturability of complex geometries with different FDM techniques (thermoplastic and ceramic paste materials).

TPMS structures are among the better performing standard 3D infills available (Qin et al., 2017), are modeled by meshing an interpolation of points distributed according to the equation approximation of TPMS surfaces within a specified domain of 0 to x Pi, for which Grasshopper, a graphical interface for parametric design is used. Experimentation consists of:

2) Compression tests and print tests to set base parameters: Volume, Scale of reliable and consistent prints.
3) Compression tests to review differences of performance between Materials and to assess differences between simulation performance and physical performance.
4) Compression tests to assess differences between base tokens and algorithmically optimized tokens.
5) Compression tests of bespoke matrices based on TPMS for optimal deformation and compression performance.

As in bone structure (Liebschner and Wettergreen, 2003; Gibson, 1985), form rigidity by shell thickness provides superior strength while foam like stochastic fibrous structures can localize deformation for energy absorption and behave roughly isotropic (Gibson and Ashby, 1999). Parametric variations of 3D infills and superficial treatment show the potential of allowing gradual transformations of the mechanical characterization of 3D printed tokens.

For the second part, the application of differentiated 3D infills in a large scale building component is evaluate in a case study. The mechanical performance of a parametrically designed (Burry, 1996) pillar built following 4 different methods for optimization are tested. Experimentation consists of:

6) Computation and Manufacturability of FEM influenced complex shapes
7) Compression test for pillar segment with constant 3D infill.
8) Compression test for pillar segment with differentiated 3D infill based in strain threshold perimeters
9) Compression test for pillar segment with differentiated polyhedral 3D infill based strain cloud
10) Compression test for pillar segment with superficial fractal ornamentation

A. Materials

Custom feedback loop and data links are required to FEM process FDM pieces, a standard workflow is yet to be developed. The generalized process proposed for this research follows:

- First Geometries are modeled in Rhinoceros 3D software.
- Infill designs developed in Grasshopper Parametrical Modelling tool with Millipede Component, calculated with Karamba FEM analysis and iterated for optimization with Galapagos plugin.
- Large scale designs simulated with SimScale cloud analysis and exported to be processed with ParaView open source software. ParaView unstructured data is imported back to Rhinoceros through Python programming language and through 3D mesh.

1) Manufacturability for thermoplastic materials

Infill tokens printed with WASP 20-40 Turbo 3D Printer with 1.75 PLA and TENAX filament. Large scale tokens printed with WASP 3MT 3D Printer with PLA pellets. Tokens printed at 190 ºC and max print speed of 100 mm/s.

Infill design is based on the following constraints:

- Continuous toolpaths and thicker than 1mm walls are considerably more reliable.
- Avoiding retract and travel operations provide higher quality pieces. Discontinuities in the fibrous structure provide the weakest connections.
- Full melting of thermoplastic is paramount for a correct cohesion of layers. If the filament or pellet line is not fully melted, the semi molten plastic, although positioned correctly, is not fused and will ultimately fail in the layer joint area.

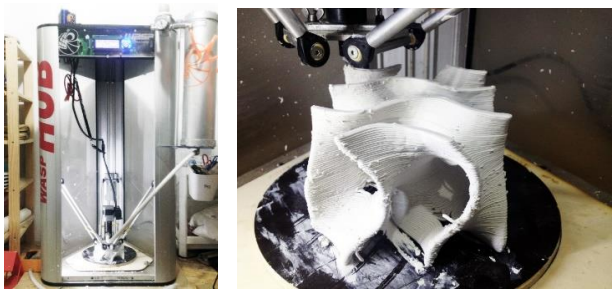

Fig. 5. WASP 2040 Turbo clay deposition.

2) Manufacturability for paste materials

Clay deposition is also tested to provide insights for a generalized technique and Automation of FEM influenced FDM processes require a manufacturability test, as geometrical constraints for deposition and material properties must be taken into account for successful reproduction.

Clay tests where manufactured in white porcelain 950/1050º distributed by Diez Ceramic, produced specially for Fused Deposition in WASP 2040 Clay 3D printer. Although production for differentiated infills is possible, manufacturing constraints limit significantly the geometrical freedom. The factors for infill design found to be most influential are:

- Impossibility to vitrify/solidify bridges during extrusion
- No secondary structure is viable
- For highly complex infill designs with overhangs of 45º to 60º angles, up to 10-15% deformation after curating in oven occurred.

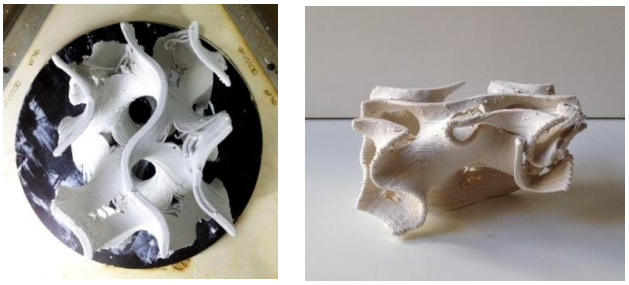

Fig. 6. Deformation of curated ceramic material.

Despite the limitations for Clay 3Dprinitng (Figure 5) FEM influenced 3D infills, the technique shows an exceptional reproduction speed and, if constraints are met, high fidelity.

Although complex geometries are correctly built, ceramic tokens showed large deformation after curation (Figure 6). Further experimentation with paste materials curation process and geometrical constraints is thus required before proceeding to mechanical analysis.

For the purpose of this research, only thermoplastic tokens are evaluated.

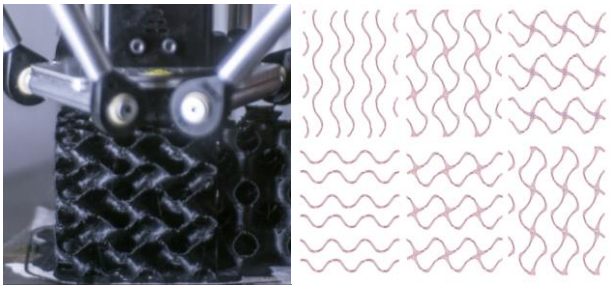

Fig. 7. A gyroid-like token with toolpath contour every 10mm.

3) Compression performance evaluation of thermoplastic building components

For the characterization of infill behavior 6cm3 infill cubic tokens where fabricated and tested: 4 standard infill, and 8 FEM influenced differentiated infill tokens. Differentiated infill tokens where developed with 2 geometrical characteristics.

For large scale application assessment, 4 iterations of a pillar building component segment where fabricated and tested.

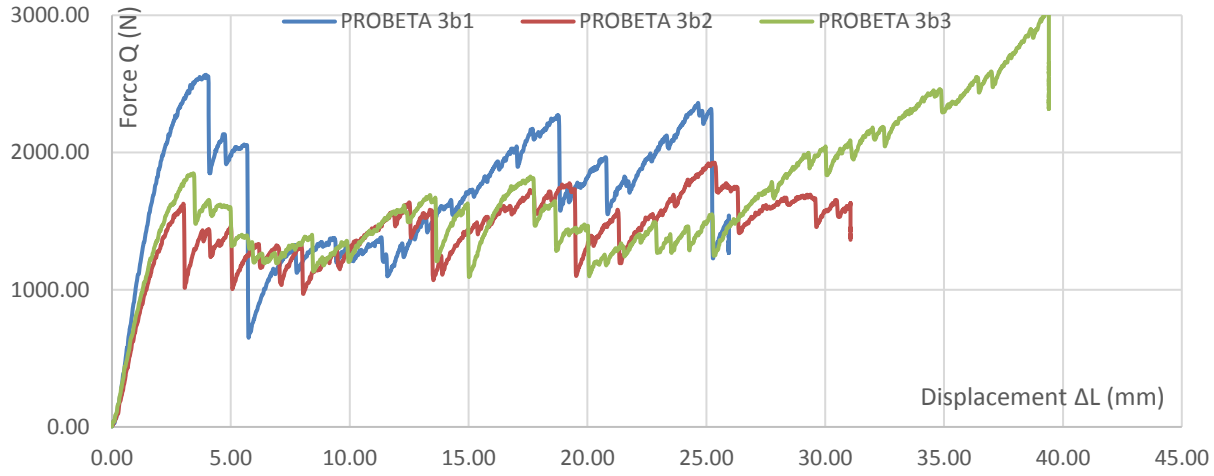

Fig. 8. TreeD PLA Gyroid-like token with non-differentiated 3D infill design force-displacement graph.

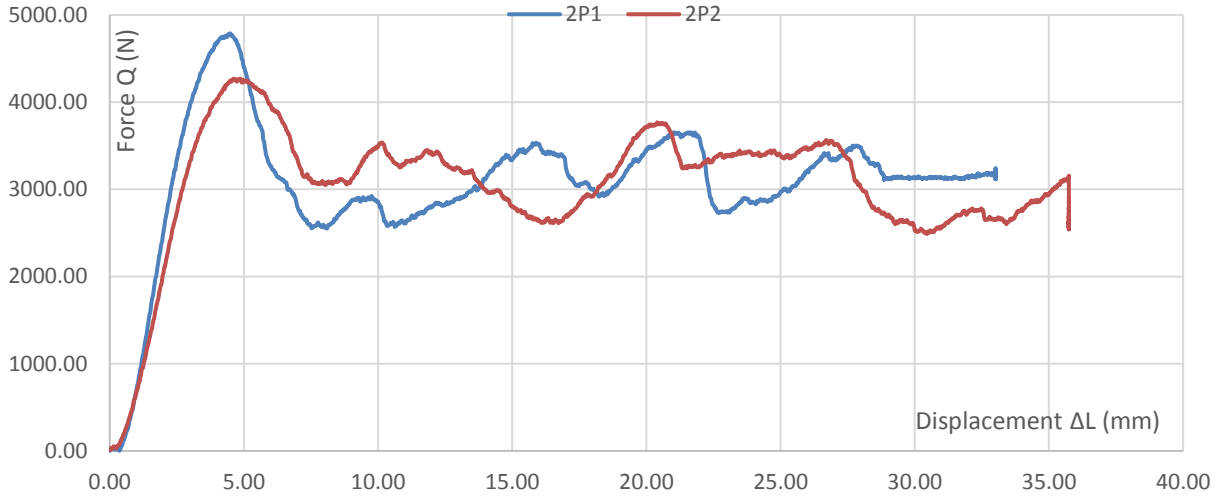

Fig. 9. TreeD TENAX Gyroid-like token with non-differentiated 3D infill design force-displacement graph.

Mechanical Tests made in the Universal Test Machine INSTRON Type, which possess a highly sensitive system for measuring load, with a load cell whose calibration and force measurement tolerance is less than 1%, full scale is 100 kN.

B. Standard gyroid infill analysis. Standard 3D infill design.

Base tokens use standard 3D infill designs provided by commercially available slicing software (Figure 7). Two different plastics are compared: Polylactic Acid and TENAX. The mechanical performance is characterized by having "camel back" humps as shown in the graphics (Figure 8 and 9). These indicate the collapse of a level corresponding to a period. After the collapse of the three levels in these base cases, the piece is compacted and starts to behave more like a solid.

1) FEM influenced FDM for differentiated infill design

TPMS have the particularity of having 0 mean curvature at every point, as in saddle shapes, this continuity if exploited by the layer by layer extrusion fabrication, for having the lightest optimum distribution of tensions with the least amount of material. For the optimization process, deformations of the TPMS matrix provides differentiation of density following the vector of displacement, thus, utilizing the tension-displacement relationship, more rigid token are built.

Fig. 10. Algorithmically differentiated token with toolpath contour every 10mm.

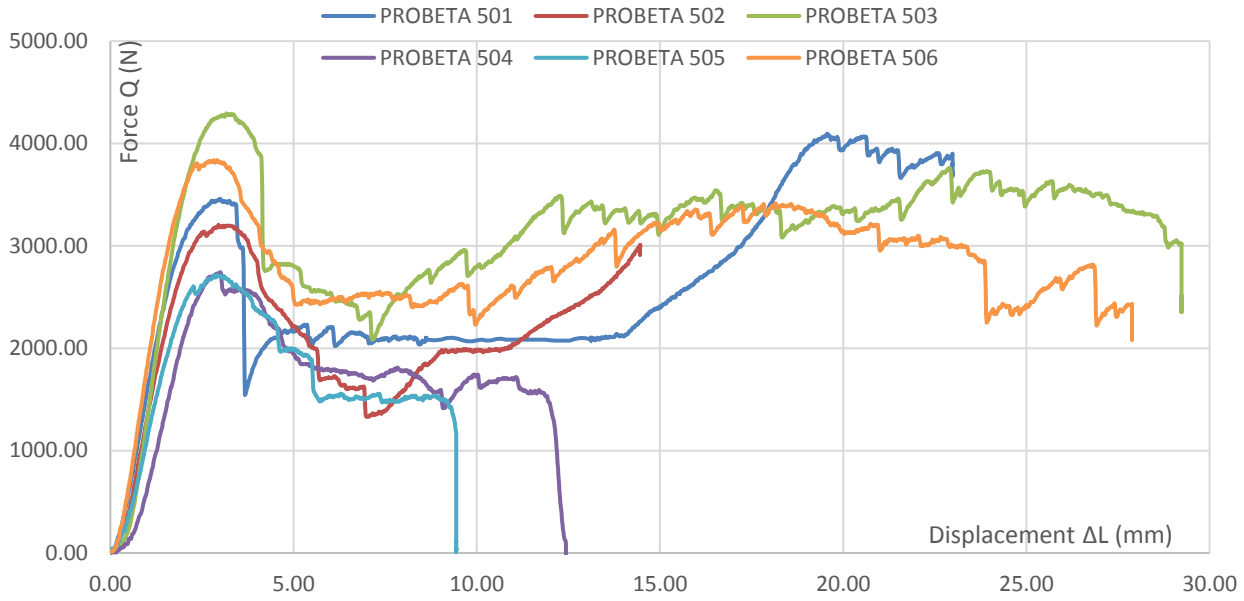

Fig. 11. FEM influenced 3D infill design and optimization with Rhinoceros 3D, Karamba and Galapagos plugins.

Optimized Tokens with the same volume and density (as per virtual model) are modeled. Manufacture shows slight variation in density (Table 1). The optimization algorithm searches for a more complex material distribution that varying the density within the volume.

TABLE I
DENSITIES COMPARISON

Class	Token	Density (g/cm³)		
		$P_{\bar{x}}$	$V_{\bar{x}}$	$D_{\bar{x}}$
2P	2P1	31	200,2	0,155
	2P2	31	224	0,138
3b	3b1	25	221,8	0,113
	3b2	23	218,9	0,105
	3b3	23	223,3	0,103
5O	5O1	27	222,5	0,121
	5O2	31	218,5	0,142
	5O3	30	218,8	0,137
	5O4	28	220,6	0,127
	5O5	28	219,5	0,128
	5O6	28	221	0,127
7b	7b1	34	226,6	0,15
	7b2	33	226,6	0,146

2) Differentiated 3D infill design to minimize deformation.

Curvature continuity is not anymore assured and density variations occur along the deposition process (Figure 10). The process of parametric transformation breaks the constant camel hump characterization (Figure 11). In the first case, optimization is constrained to within 6Pi period of gyroid geometry. Only pushing base infill design to the areas where superior strain is to be expected according to the simulation.

3) Differentiated 3D infill design to maximize energy absorption.

The base geometry for this case is transformed without the periodic constrain of 6 Pi. A sponge-like geometry is created by taking the parametric transformations to the minimum scale of 0.4mm of deposition according to the nozzle size (Figure 12). A slow, continuous thin flow of thermoplastic provides a general stochastic interconnection of fibers.

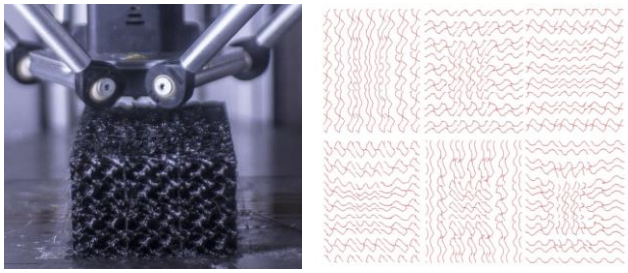

Fig. 12. Algorithmically differentiated token with toolpath contour every 10mm.

Tokens present an Energy Absorption similar to that of Foams and commence to behave solids as it is continuously compacted by deformation (Figure 13).

C. FEM influenced FDM Large Scale implementation of differentiated 3D infills.

For the second part of the research, the use of pellet extruders is used in the application of mechanically characterized infill application to building components. The deposition system is in

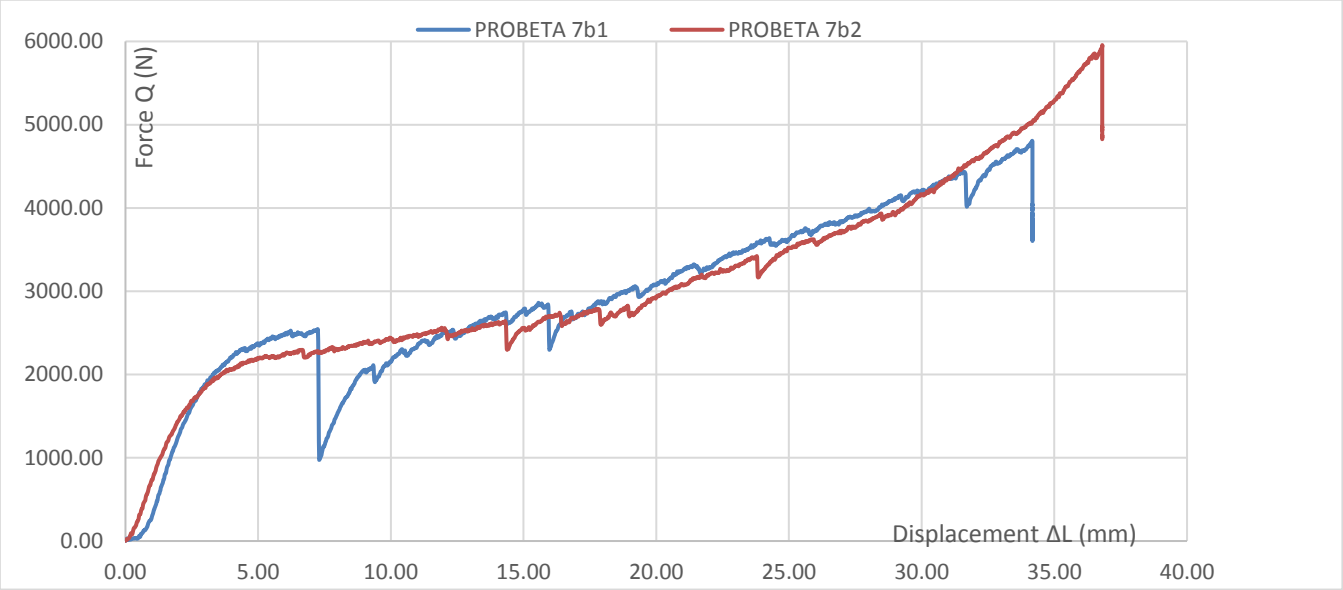

Fig. 13. Differentiated 3D infill design force-displacement graph.

general terms maintained, a Numeric Control system moves a deposition mechanism following a coordinate system that was computationally designed. The main difference for this large scale application is the width of walls constrained by nozzle extrusion diameter of a 3mm. A computational workflow and manufacture technique tailored for large scale application are presented. FEM analysis in this case is simplified to a lesser computationally expensive workflow, in order to produce viable results.

1) Computational workflow for FEM influenced FDM for optimized global geometry design. A case Study

FEM influenced FDM is particularly relevant for the production of singular instances of performative (Kolarevic, 2003) and parametric models (Burry, 1996) in digital design (Willmann et al., 2013) due to their intrinsic complexity

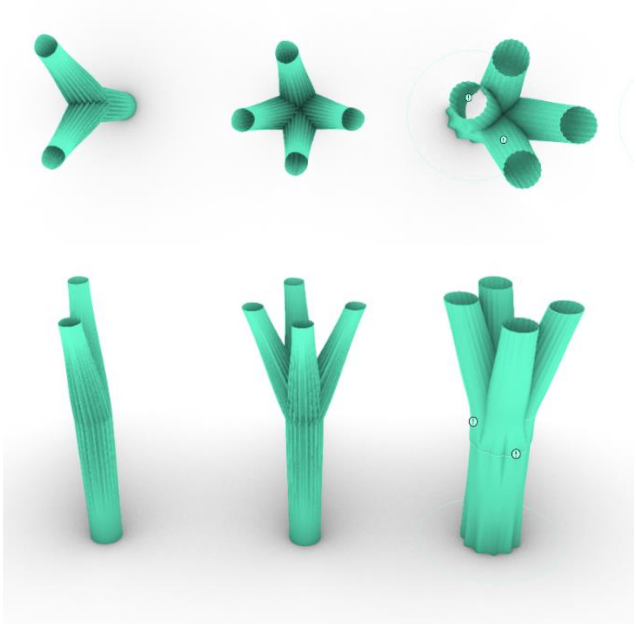

Fig. 14. Algorithmically designed Pillar with parametric branching, angle and shell ornamentation.

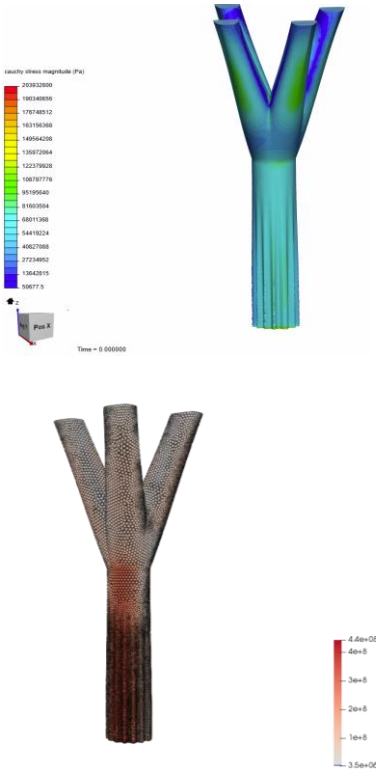

Fig. 15. VTK FEM simulation results produced with SIMSCALE are discretized with PARAVIEW software for Indexing and Processing in Rhino/Grasshopper.

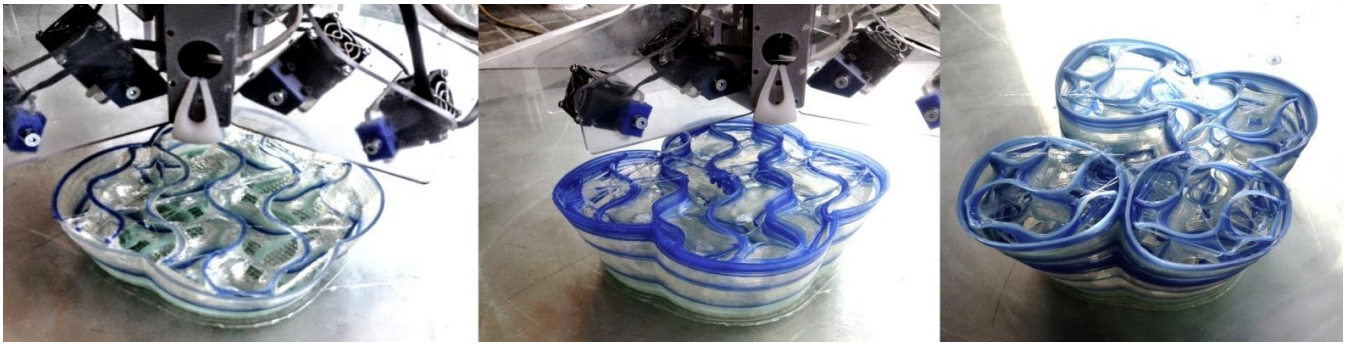

Fig. 16. Pillar segment with 10% Density, constant

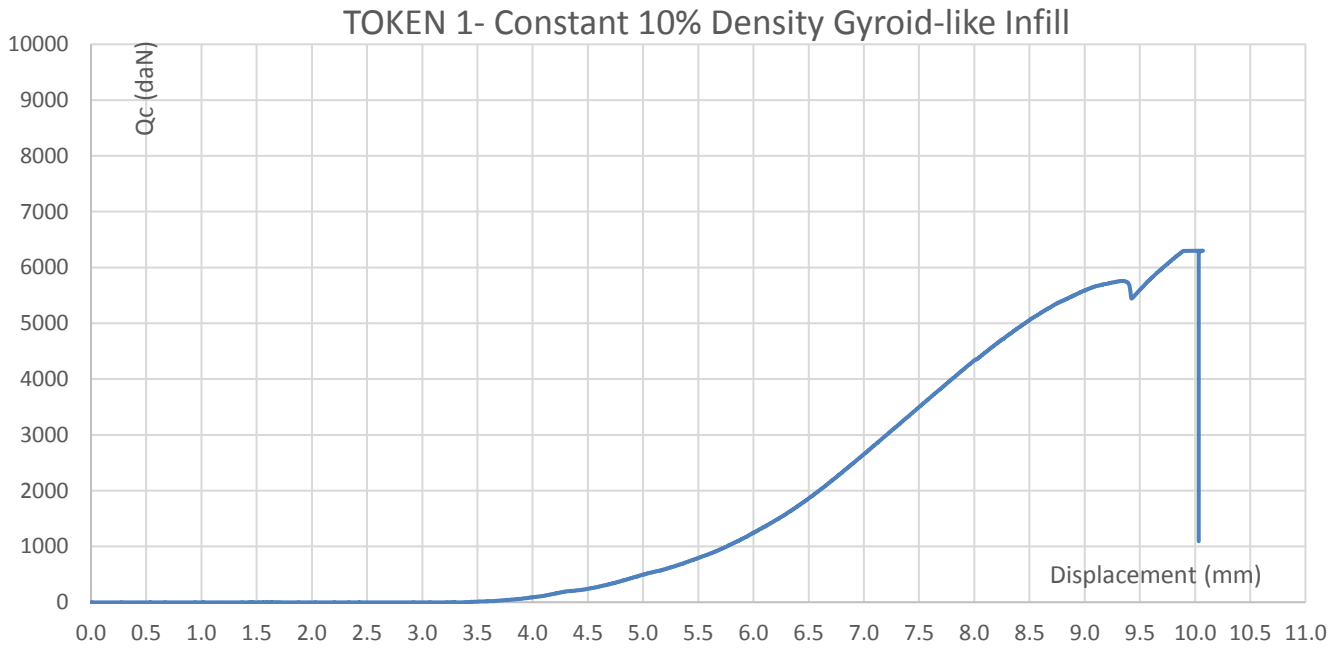

Fig. 17. Force-displacement graph.

(Dillenburger and Hansmeyer, 2013; Carpo, 2012). A set of parametrically design branching structures (Figure 14) is modeled and fabricated for the purpose of testing variable matrices and infill mechanical performance.

This branching structure is discretized in external cloud based simulation SimScale. The discretization process is based on 3D mesh generating system common for Fuild Dynamics simulations. This 3D mesh provides a system for indexing stress values in 3D space (Figure 15) accessible through Visualization Toolkit (VTK).

In order to structure and successfully map FEM values to custom 3D infill gCode toolpath these values must necessarily organized in discrete units. This research studies discretized values organized in two procedures through OpenFoam based software ParaView: first, a high resolution unstructured grid of VTK cells (Pham and Dimov, 2001) processed by a color gradient in a 3d Glyph placeholder in space and a second less computationally expensive, and thus lower resolution, through establishing thresholds of strain, and organize isovolumes of low to high strain.

2) Density differentiation design, manufacturability and mechanical performance evaluation of large scale components

For the purpose of comparing the compression performance of different geometrical iterations, the most complex segment of the pillar is studied in detail and manufactured using 4 different approaches. Each piece is designed to weight roughly 1 kg and to be manufactured in about 2 hours.

III. RESULTS

A. *Token 1 Constant density infill manufacture*

It is processed with commercially available software. An infill of 10% density based on gyroid-like pattern is applied. Results of this process can be seen in figure 16 and figure 17.

B. Token 2- FEM influenced Variable density infill token manufacture

It is processed with FEM software first. The unstructured data set is then segmented into differentiated thresholds based on strain levels, providing a clear limit of behavioral characterization. A different density of gyroid-like geometries is infilled, so that higher density of infill corresponds to volumes where more strain is expected. Each von-mises strain cloud is exported to commercially available slicing software Slic3r and the standard density variation method is used to produce the final piece (Figure 18). This process is adapted to recreate a computationally viable method approximated to applying the second characterization behavior presented previously. We show pillar segment with 5% - 10% - 15% density in figure 19 and the force-displacement graph in figure 20.

C. Token 3- FEM influenced polyhedral infill token manufacture

It is processed with FEM first, as in token 2, the unstructured data from VTK cells is organized into strain thresholds, with the fundamental difference that instead of using the perimeter

Fig. 18. Detail View of unstructured discretized individual values at full resolution divided into 3 isostatic cloud thresholds, low strain, mid strain, high strain.

Fig. 19. Pillar segment with 5% - 10% - 15% Density, constant.

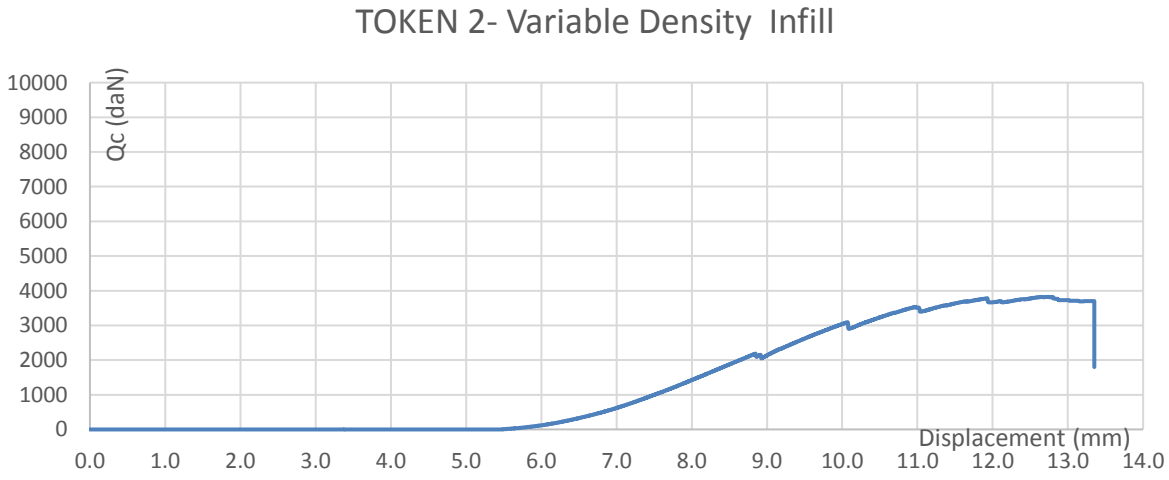

Fig. 20. Force-displacement graph.

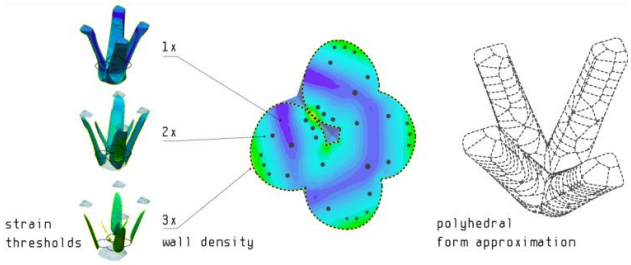

Fig. 21. Detail View of cellular (polyhedral) population based on FEM values in isostatic cloud thresholds.

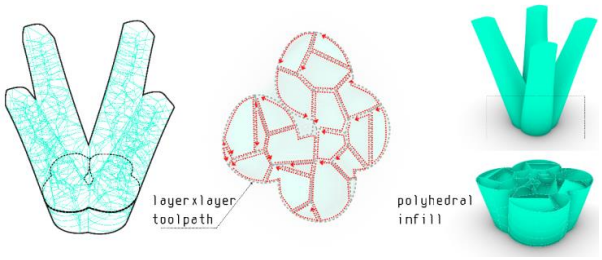

Fig. 22. Detail View continuous toolpath creation. The isostatic cloud threshold perimeter does not interrupt deposition process.

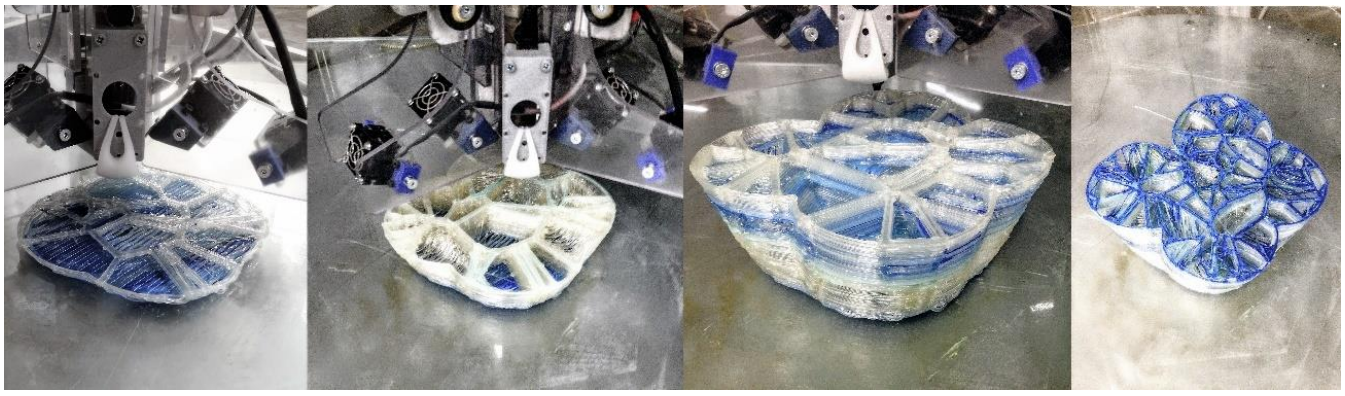

Fig. 23. Pillar segment with polyhedral infill.

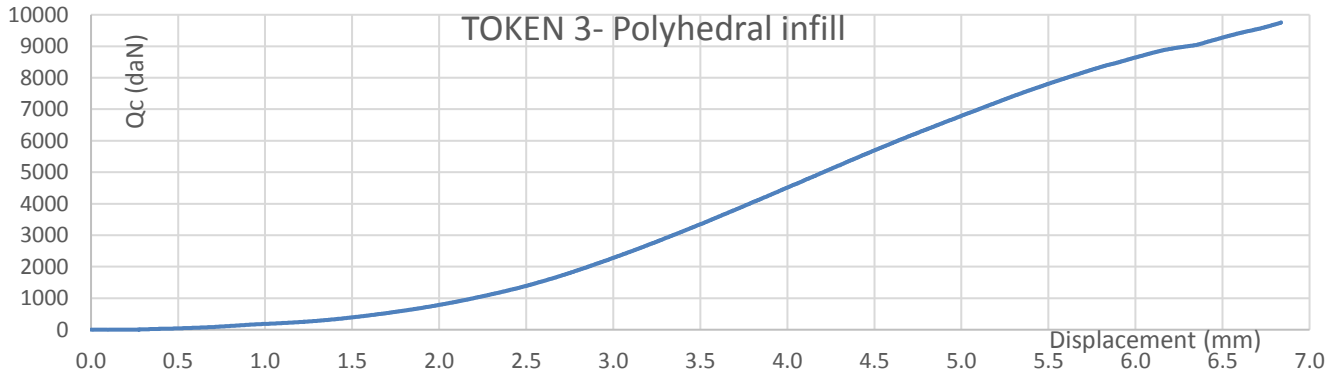

Fig. 24. Force-displacement graph.

Fig. 25. Parametric surface patterning.

of the isostatic cloud threshold as a geometrical limit, continuity is assured by using a system of polyhedral approximation, in this case through population of points converted into 3D voronoi cells. So, the cloud thresholds must be processed in Rhinoceros again, to recreate a polyhedral aggregation approximation of the original geometry (Figure 21).

The global shape is formed by an aggregation of individual polyhedral cells, producing an overall augment of density where simulation indicates more strain by multiplying the amount of cells, therefore, walls produced, emulating bone construction. The design maintains deposition and thus fiber

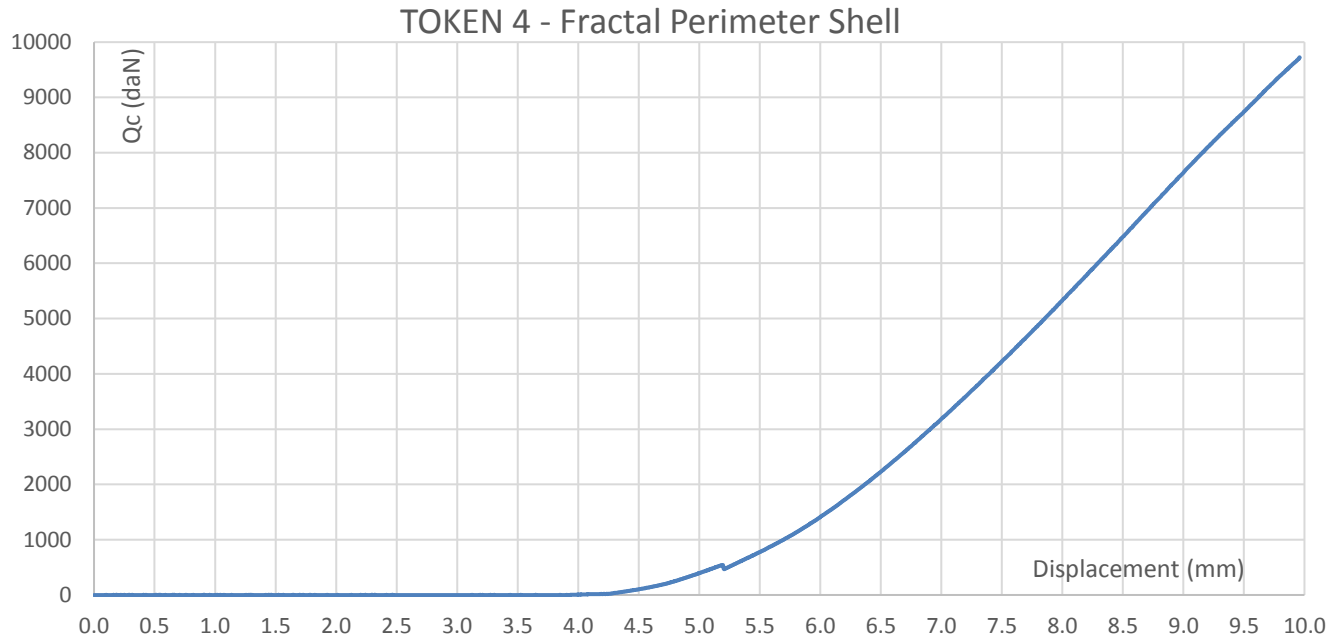

Fig. 26. Force-displacement graph.

continuity within each of the cells along the layer by layer deposition process (Figure 22).

Pillar segment with polyhedral infill can be seen in figure 23 and force-displacement graph in figure 24.

D. Token 4 - Surface patterning approach

It takes the complementary approach of patterning the surface to provide superior stiffness to the structure. This is achieved by breaking into fractal segments the original perimeter of the surface (Figure 25). The perimeter in the base is continuously segmented along its growth in height, and is

Fig. 27. Failure detail of token 1.

manufactured with a constant 3 mm wall thickness. In order to evaluate the potential of surface patterning in augmenting resistance no infill is applied and the results can be seen in figure 26.

E. Compression Performance

The constant density pattern shows a dramatic failure and decrease in resistance, without previous noticeable deformation or fracture (Figure 27).

The variable density pattern shows a continuously increasing failure, with accumulation of fractures once the form is considerably deformed. The areas of fracture are very low density volumes and points of discontinuity between the differentiated geometries (Figure 28). The discontinuous toolpath design results in a considerably poorer weaker component.

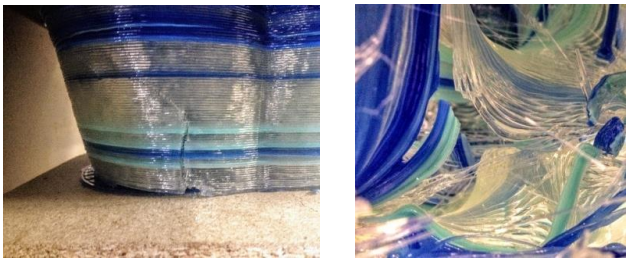

Fig. 28. Failure detail of token 2.

F. Infill tests results

While the number of tests conducted is not enough to be statistically conclusive, the preliminary results suggest nevertheless that optimization of specimens through the proposed workflow can lead to improved structural behavior compared to the initial non-optimized specimens.

Polyhedral infill and fractal transformation of the perimeter showed exceptional resistance to deformation (Figure 29) and sustained the 10 T applied, limited by the measuring equipment. The polyhedral infill token weights considerably more (1.4 kg)

Fig. 29. Minimal deformation and improved strength in polyhedral cell and fractal shell tests.

than the rest of the iterations since custom made gCode is particularly susceptible to discrepancies (Table 2). Better tools for calculating final pieces mechanical and geometrical characteristics of custom made infills are to be developed.

Both experimental and simulation results demonstrate the benefit of material redistribution by optimization as seen in the improved compression performance.

Similarly, the combined benefits of domain optimization eliminate the problem of hump like deformation behavior and shows potential in the design of Additively Manufactured spongy lattices which their solid like behavior is triggered as deformed. A designed anisotropy shows great potential in the performance improvement of fibrous components by introducing controlled complex deformation behaviors.

IV. DISCUSSION

Commercially available Slicing software (Cura, Slic3r) include undifferentiated 3D infills, interesting for their better mechanical properties as compared to continuous vertical extrusion of patterns in 2D solutions. These geometrical designs present yet some challenges for successful FEM simulation, as some of the manufacturability aspects.

The characterization of mechanical behavior in functionally graded components how several potentials in maximizing performance of building component manufactured with FDM techniques.

Regarding 3D Infill geometry performance:

- By adapting the geometry and overall density, FDM processes potentially produce highly differentiated mechanical properties for functionally graded building components, with no need of changing material.
- Foams manufactured with FDM — roughly isotropic — can absorb energy from any direction with the capacity to undergo large deformation at constant σ.
- Varying the deposition toolpath to control differentiated density infill based on FEM results and deformation vectors may provide stiffness and increase in compression performance.

TABLE 2
CASE STUDY RESULTS

	DATA			RESULTS			
Token	**Description**	**Weight (G)**	**H (mm)**	**H dis (mm)**	**H Difference (mm)**	**Qc max (daN)**	**Failure**
1	Constant Density Infill	982	126	117,5	8,5	6301	Yes
2	Variable Density Infill	1222	124	123,0	1,0	3824	Yes
3	Polyhedral Infill	1403	101	101,0	0,0	9758	No
4	Fractal Perimeter Shell	1109	122	122,0	0,0	9725	No

Regarding large scale application performance:

- The mechanical behavior of building components produced with standard deposition techniques, even with 3D infill designs, can be significantly improved by applying FEM influenced infill and by increasing stiffness by surface ornamentation
- Geometrical discontinuity in varying density infills influenced negatively the resistance of tokens. Further tests should consider the more important aspect of fiber continuity over the augment of density in higher strain areas.
- Continuity of deposition, layer through layer and within each section if paramount for maximizing compressive strength.

ACKNOWLEDGEMENTS

Special thanks to Daniel García and Ignacio Prieto from Fab Lab Istituto Europeo di Design (IED Madrid) for the support and advice in the development and fabrication of test tokens.

This research was supported by Consejo Nacional de Ciencia y Tecnología (CONACYT Mexico) and by Fab Lab Istituto Europeo di Design. Mechanical Analysis developed at Laboratorio Docente de Elasticidad y Resistencia de Materiales, Escuela Técnica Superior de Ingenieros Industriales, Universidad Politécnica de Madrid.

REFERENCES

Ahn, S. et al, (2002). "Anisotropic material properties of fused deposition modeling ABS," Rapid Prototyping Journal, vol. 8, (4), pp. 248-257.

Burry, M. (1996). "Parametric design and the Sagrada Familia," Architectural Research Quarterly, vol. 1, (04), pp. 70-81.

Carpo, M. (2012). "Digital darwinism: mass collaboration, form-finding, and the dissolution of authorship," Log, (26), pp. 97-105. Available: https://www.jstor.org/stable/41765764.

Carpo, M. (2017). The Second Digital Turn: Design Beyond Intelligence. MIT Press.

Dillenburger, B. and Hansmeyer, M. (2013). "The resolution of architecture in the digital age," in CAAD Futures 2013. Communications in Computer and Information Science, pp. 347-357.

Gibson, L. (1985). The mechanical behaviour of cancellous bone," J. Biomech., vol. 18, (5), pp. 317-328. DOI: 10.1016/0021-9290(85)90287-8.

Gibson, L. and Ashby, M. (1999). Cellular Solids: Structure and Properties. Cambridge university press.

Gospill, J. A., Shindler, J. and Hicks, B. J. (2017)."Using finite element analysis to influence the infill design of fused deposition modelled parts," Progress in Additive Manufacturing.

Kolarevic, B. (2003). Architecture in the Digital Age. New York: Spon Press.

Liebschner, M. and Wettergreen, M. (2003). "Bone," in Topics in Tissue Engineering, N. Ashammakhi and P. Ferretti, Eds. University of Oulu.

Malé, M. (2016). "El Potencial De La Fabricación Aditiva En La Arquitectura : Hacia Un Nuevo Paradigma Para El Diseño Y La Construcción." , Universitat Politècnica de Catalunya.

Oxman, N. and Rosenberg, J. L. (2007). "Material-based Design Computation An Inquiry into Digital Simulation of Physical Material Properties as Design Generators," International Journal of Architectural Computing (IJAC), pp. 26-44.

Pham, D. T. and Dimov, S. S. (2001). Rapid Manufacturing.

Qin, Z. et al. (2017). "The mechanics and design of a lightweight three-dimensional graphene assembly," Science Advances, vol. 3, (1), pp. e1601536. Available: https://www.ncbi.nlm.nih.gov/pubmed/28070559. DOI: 10.1126/sciadv.1601536.

Tam, K. M. and Mueller, C. T. (2017). "Additive Manufacturing Along Principal Stress Lines," 3D Printing and Additive Manufacturing, vol. 4, (2), pp. 63-81.

Willmann, J. et al. (2013). "Digital by material," in Rob | Arch 2012, pp. 12-27.

Yoo, D. J. (2011). "Porous scaffold design using the distance field and triply periodic minimal surface models," Biomaterials, vol. 32, (31), pp. 7741-7754. Available: https://www.clinicalkey.es/playcontent/1-s2.0-S0142961211007903. DOI: 10.1016/j.biomaterials.2011.07.019.